ELSEVIER

Journal of Alloys and Compounds 408–412 (2006) 27–32

Journal of ALLOYS AND COMPOUNDS

www.elsevier.com/locate/jallcom

Change of the electronic states in $CeIn_3$, $CeRhIn_5$ and $CePt_3Si$ tuned by pressure

Y. Ōnuki[a,*], R. Settai[a], H. Shishido[a], T. Kubo[a], Y. Yasuda[a], K. Betsuyaku[b], H. Harima[c]

[a] *Graduate School of Science, Osaka University, Toyonaka, Osaka 560-0043, Japan*
[b] *Electronics and Photonics Technologies, Science and Technology, Fuji Research Institute Corporation, 2-3 Kanda-nishikicho, Chiyoda-ku, Tokyo 101-8443, Japan*
[c] *Department of Physics, Kobe University, Kobe 657-8501, Japan*

Available online 23 June 2005

Abstract

We have studied a change of the electronic states in antiferromagnets $CeIn_3$, $CeRhIn_5$ and $CePt_3Si$ via the de Haas–van Alphen experiments. The critical pressure P_c, where the Néel temperature becomes zero, is $P_c \simeq 2.5$ GPa in $CeIn_3$ with the cubic crystal structure, in which the narrow pressure region superconductivity appears below a superconducting transition temperature $T_{sc} = 0.2$ K. In the pressure region $P > P_c$, we detected a main Fermi surface with the cyclotron mass $m_c^* = 53m_0$, which most likely corresponds to a nearly spherical Fermi surface in the paramagnetic state, namely a 4f-itinerant Fermi surface. The Fermi surface in the antiferromagnet $CeRhIn_5$ with the tetragonal crystal structure is similar to that of $LaRhIn_5$, consisting of two kinds of nearly cylindrical Fermi surfaces. We observed a drastic change of the Fermi surface from 4f-localized ($LaRhIn_5$) to 4f-itinerant ($CeCoIn_5$) Fermi surfaces at $P_c \simeq 2.4$ GPa. The cyclotron mass increases intensively above 1.6 GPa where superconductivity sets in. $CePt_3Si$ with the tetragonal crystal structure without inversion symmetry is highly different from $CeIn_3$ and $CeRhIn_5$ in magnetism and superconductivity. It orders antiferromagnetically below $T_N = 2.3$ K and becomes superconductive below $T_{sc} = 0.6$ K at ambient pressure. With increasing pressure, the cyclotron mass is found to be reduced, together with a steep decrease of T_N and T_{sc}, where P_c is most likely about 1.5 GPa in $CePt_3Si$. The heavy fermion state of $CePt_3Si$ is realized at ambient pressure.

Keywords: de Haas–van Alphen effect; Superconductivity; Heavy fermion state; $CeIn_3$; $CeRhIn_5$; $CePt_3Si$

1. Introduction

The 4f electron of cerium compounds exhibits a variety of characteristic features including magnetic and charge orderings, spin and valence fluctuations, heavy fermions and anisotropic superconductivity. The electronic states in the cerium compounds, where the Ruderman–Kittel–Kasuya–Yosida (RKKY) interaction and the Kondo effect compete each other, can be tuned by pressure. When pressure P is applied to the cerium compounds with antiferromagnetic ordering such as $CeIn_3$ and $CeRhIn_5$, the Néel temperature T_N decreases, and a quantum critical point corresponding to the extrapolation $T_N \to 0$ is reached at $P = P_c$ [1–4]. Surprisingly, superconductivity and/or the non-Fermi liquid nature appear around P_c. Crossover from the magnetically ordered state to the non-magnetic state under pressure is currently the most interesting issue in the cerium compounds.

We have studied a change of the electronic states in antiferromagnets $CeIn_3$, $CeRhIn_5$ and $CePt_3Si$ via the de Haas–van Alphen (dHvA) experiments under pressure. The electronic states, which are tuned by pressure, have been investigated via challenging dHvA experiments. The present paper reports the dHvA results at high pressures up to 3 GPa, indicating a drastic change of the Fermi surface properties. A relation between superconductivity and the Fermi surface properties has been also investigated.

2. Experimental

Single crystals were grown by the Czochralski pulling method in an rf-furnace for $CeIn_3$, the In-flux method for

* Corresponding author. Tel.: +81 6 6850 5368; fax: +81 6 6850 5372.
E-mail address: onuki@phys.sci.osaka-u.ac.jp (Y. ¯Onuki).

0925-8388/$ – see front matter © 2005 Elsevier B.V. All rights reserved.
doi:10.1016/j.jallcom.2005.04.101

$CeRhIn_5$, and the Bridgeman method and mineralization for $CePt_3Si$ [5–7]. The residual resistivity ratio RRR (=ρ_{RT}/ρ_0, ρ_{RT} is the electrical resistivity at room temperature, ρ_0 is the residual resistivity) is 90 in $CeIn_3$, 330 in $CeRhIn_5$ and 106 in $CePt_3Si$, indicating high-quality samples.

The dHvA experiments were done by the standard field modulation method with a modulation frequency of 3.5 Hz and a modulation field of 80 Oe. Pressure was applied by utilizing an MP35N piston cylinder cell with a 1:1 mixture of commercial Daphne oil (7373) and kelosene, and calibrated by the superconducting transition temperature of Sn.

3. Experimental results and discussion

3.1. $CeIn_3$

$CeIn_3$ with the $AuCu_3$-type cubic crystal structure is a well-known Kondo-lattice compound with antiferromagnetic ordering at 10 K. With increasing pressure, the Néel temperature decreases and becomes zero around 2.5 GPa. The critical pressure is $P_c \simeq 2.5$ GPa, in which the narrow pressure region superconductivity appears below T_{sc}=0.2 K [1,3].

We carried out the dHvA experiment under pressure. The detected dHvA signal V_{osc} for the magnetic field H is simply written as follows:

$$V_{osc} = A \sin\left(\frac{2\pi F}{H} + \phi\right),$$

where the dHvA frequency F (=$\hbar S_F/2\pi e$), which is expressed as a unit of magnetic field, corresponds to the extremal (maximum or minimum) cross-sectional area of the Fermi surface S_F. From the temperature dependence of the dHvA amplitude A, we can determine the cyclotron effective mass m_c^*.

Figs. 1 and 2 show the pressure dependence of dHvA frequency F and cyclotron mass m_c^* for the magnetic field H along ⟨1 1 0⟩. The dHvA frequency for branch "d" increases slightly with increasing pressure. The similar pressure dependence of the cyclotron mass is also observed: $m_c^* = 17m_0$ at ambient pressure, and $20m_0$ at 2.4 GPa for branch "d". Interesting is that branch "a", which is observed at 2.7 GPa, possesses an extremely large cyclotron mass $m_c^* = 53m_0$. Branch "a" is the main Fermi surface, which is not observed below $P_c \simeq 2.5$ GPa. An appearance of branch "a" indicates that $CeIn_3$ becomes paramagnetic.

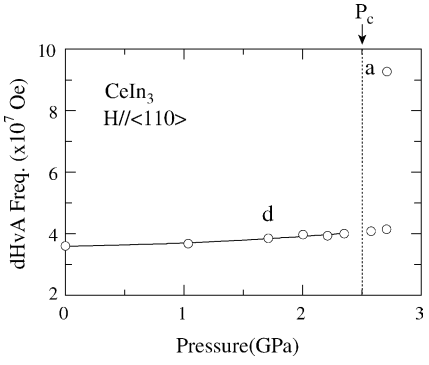

Fig. 1. Pressure dependence of the dHvA frequency in $CeIn_3$.

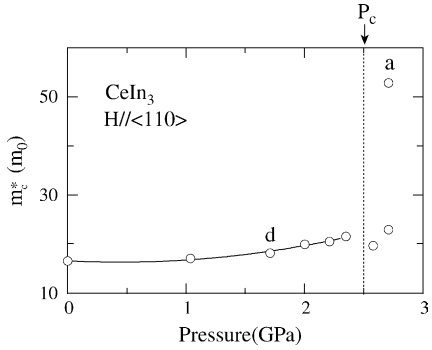

Fig. 2. Pressure dependence of the cyclotron mass in $CeIn_3$.

To clarify the origin of the dHvA branches, we show in Fig. 3 the Fermi surface in $LaIn_3$, which was calculated by the FLAPW method. The Fermi surface consists of a complicated band 6 hole-Fermi surface and a nearly spherical band 7 electron-Fermi surface. The former Fermi surface consists of three kinds of major parts, which are centered at Γ, R and X points. Among them, a Fermi surface centered at Γ, denoted by "d", is electron in dispersion and is spherical in topology, bulges slightly along ⟨1 0 0⟩ and possesses a slender arm along ⟨1 1 1⟩.

As discussed in Refs. [5,8], the Fermi surface of $CeIn_3$ at ambient pressure is approximately similar to that of $LaIn_3$, although it is strongly modified by the magnetic Brillouin zone boundaries. The dHvA frequency of branch "d", observed experimentally in the whole angle region, is in good agreement with the theoretical branch "d" of $LaIn_3$ in magnitude, although branch "d" in $CeIn_3$ corresponds to a nearly spherical Fermi surface, not possessing the slender arm along ⟨1 1 1⟩ as in $LaIn_3$ and is slightly large in volume of the Fermi surface compared to $LaIn_3$. In the case of $LuIn_3$, the topology of the corresponding Fermi surface is nearly spherical, possessing no arms. This Fermi surface corresponds to branch "d" of $CeIn_3$.

A spherical electron Fermi surface in band 7, denoted by "a" in $LaIn_3$, is not observed at ambient pressure in $CeIn_3$,

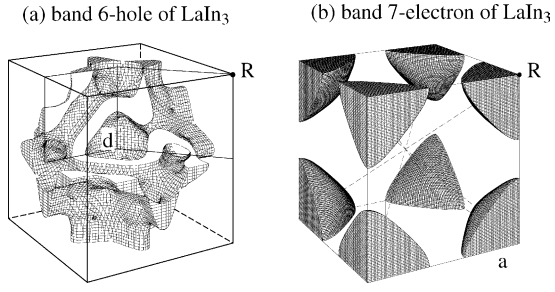

Fig. 3. Theoretical Fermi surfaces in $LaIn_3$.

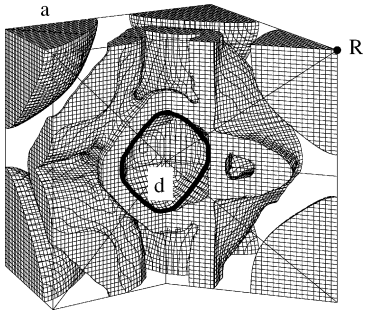

Fig. 4. Band 7 electron-Fermi surface in $CeIn_3$, calculated on the basis of the 4f-itinerant band model.

which is ascribed to the influence of the magnetic Brillouin zone boundaries. A large spherical Fermi surface named "a" also exists in the case where the 4f electron in $CeIn_3$ becomes itinerant. Fig. 4 shows the band 7 electron-Fermi surface based on the 4f-itinerant band model [9]. The theoretical dHvA frequency of branch "a" is $F = 6.84 \times 10^7$ Oe for $LaIn_3$, while it is 8.50×10^7 Oe for the 4f-itinerant band model for $H \parallel \langle 1\,1\,0 \rangle$. The detected dHvA frequency of 9.34×10^7 Oe is close to the itinerant one.

For branch "d", similar values for experiment and theory are found as well. The theoretical dHvA frequency for $LaIn_3$ is $F = 2.54 \times 10^7$ Oe for $\langle 1\,0\,0 \rangle$ and 2.29×10^7 Oe for $\langle 1\,1\,1 \rangle$, while $F = 2.20 \times 10^7$ Oe for $\langle 1\,0\,0 \rangle$, 2.38×10^7 Oe for $\langle 1\,1\,0 \rangle$ and 2.11×10^7 Oe for $\langle 1\,1\,1 \rangle$ for the 4f-itinerant band model. This is a reason why a change of the dHvA frequency of branch "d" is not observed clearly above and below P_c: 3.59×10^7 Oe at 0 GPa, 3.97×10^7 Oe at 2.0 GPa and 4.19×10^7 Oe at 2.7 GPa for branch "d" for $\langle 1\,1\,0 \rangle$ experimentally.

From these experimental results, it is concluded that a change of the Fermi surface from 4f-localized to 4f-itinerant occurs when pressure crosses $P_c \simeq 2.5$ GPa. Superconductivity appears in a narrow pressure region $\Delta P_c \simeq 0.5$ GPa around P_c. From the NQR experiment, it is clarified that a pressure-induced phase separation of antiferromagnetism and paramagnetism occurs and superconductivity coexists with antiferromagnetism in the pressure region from 2.28 to 2.5 GPa [3]. On the other hand, superconductivity is also realized in the paramagnetic state above $P_c \simeq 2.5$ GPa, following the Fermi liquid relation.

3.2. *CeRhIn*$_5$

$CeTIn_5$ (T: Co, Rh and Ir) crystallizes in the tetragonal crystal structure. The uniaxially distorted $AuCu_3$-type layers of $CeIn_3$ and the TIn_2 layers are stacked sequentially along the [0 0 1] direction (c-axis). $CeCoIn_5$ and $CeIrIn_5$ reveal superconductivity at ambient pressure [10], whereas $CeRhIn_5$ orders antiferromagnetically below T_N=3.8 K [2,11,12]. With increasing pressure, the Néel temperature in $CeRhIn_5$ increases, has a maximum around 1 GPa, and decreases with further increasing pressure. A smooth extrapolation indicates

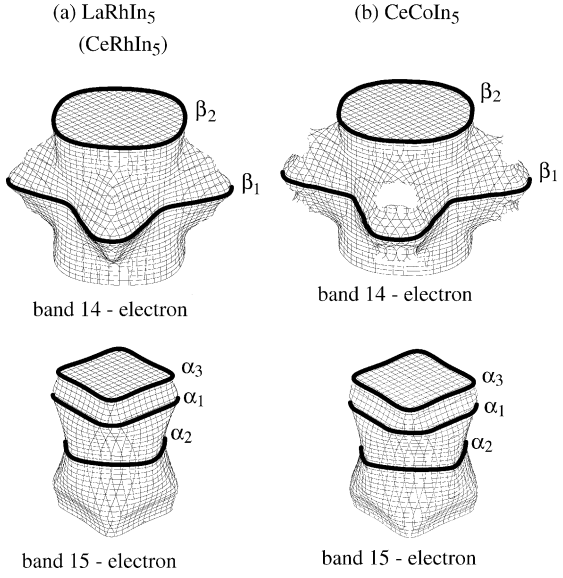

Fig. 5. Theoretical Fermi surfaces in (a) $LaRhIn_5$ ($CeRhIn_5$) and (b) $CeCoIn_5$. Small Fermi surfaces are not shown.

$T_N \to 0$ around a pressure $P = 2.3$–2.5 GPa. $CeRhIn_5$, however, reveals superconductivity in a wide pressure region from $P^* = 1.6$–5.2 GPa. Its transition temperature has a maximum around 2.3–2.5 GPa, with T_{sc}=2.2 K. This pressure of 2.3–2.5 GPa is supposed to be a critical pressure P_c in $CeRhIn_5$, where the antiferromagnetic state is changed into a paramagnetic state and also the heavy fermion state is most likely realized in this compound.

The topology of main Fermi surfaces in the antiferromagnet $CeRhIn_5$ is nearly cylindrical, and is found to be approximately the same as that of a non-4f reference compound $LaRhIn_5$, as shown in Fig. 5(a), indicating that the 4f electron in $CeRhIn_5$ is localized and does not contribute to the volume of the Fermi surfaces [6]. On the other hand, main Fermi surfaces in $CeCoIn_5$ without magnetic ordering are also nearly cylindrical but are identified by the 4f-itinerant band model, as shown in Fig. 5(b) [6,13]. The topology of the two kinds of cylindrical Fermi surfaces of $CeCoIn_5$ is similar to that of $CeRhIn_5$, but one 4f-electron in each Ce site becomes a conduction electron in $CeCoIn_5$. The detected cyclotron masses of 5–$87m_0$ in $CeCoIn_5$ are extremely large, reflecting a large γ value of 1000 mJ/K^2 mol [10,13,14]. It is noted that the "d" electrons in the T atom hybridize with the 5p electrons of In in $CeTIn_5$ and also $LaTIn_5$, which results in a small density of states around the Fermi energy. This means that there are very few conduction electrons in the TIn_2 layer and hence the Fermi surface mainly consists of the two kinds of cylindrical Fermi surfaces shown in Fig. 5.

To elucidate a change of the Fermi surface properties under pressure, we show in Figs. 6 and 7 the pressure dependence of the dHvA frequency and the cyclotron mass, respectively. The dHvA frequencies for the main dHvA branches named β_2, α_1 and $\alpha_{2,3}$, together with branches named a, b and c, in Fig. 6 are approximately unchanged up to about 2.3 GPa, as

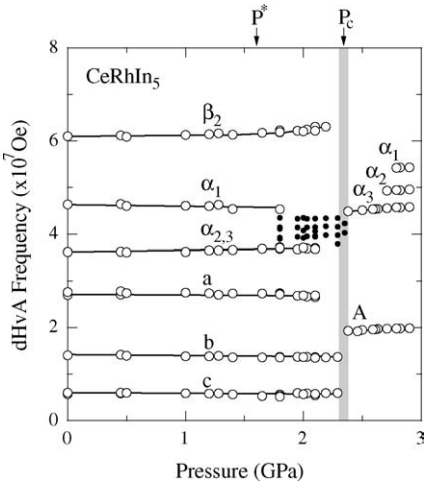

Fig. 6. Pressure dependence of the dHvA frequency in $CeRhIn_5$.

reported previously, although the previous experiments were carried out up to 2.1 GPa [12]. These branches, however, disappear completely at 2.35 GPa, and another two branches with $F = 4.23 \times 10^7$ Oe ($m_c^* \simeq 30m_0$) and 4.03×10^7 Oe ($20m_0$) appear at 2.35 GPa. We note that these branches appear from 1.8 to 2.35 GPa, which are shown by small closed circles in Fig. 6. The origin of these branches are unknown.

Above 2.4 GPa, new dHvA branches named α_i ($i = 1$–3) and A appear: $F = 5.43 \times 10^7$ Oe ($m_c^* = 23m_0$) in α_1, 4.96×10^7 Oe ($30m_0$) in α_2, 4.58×10^7 Oe ($24m_0$) in α_3 and 1.98×10^7 Oe ($9m_0$) in branch A at 2.9 GPa. The dHvA frequencies of branches α_i are larger than those below 2.4 GPa, but are approximately the same as those of $CeCoIn_5$ at ambient pressure: $F = 5.56 \times 10^7$ Oe ($m_c^* = 15m_0$) in α_1, 4.53×10^7 Oe ($18m_0$) in α_2 and 4.24×10^7 Oe ($8.4m_0$) in α_3 in $CeCoIn_5$. The present dHvA data indicate that the 4f electron becomes itinerant and significantly contributes to the volume of the Fermi surface.

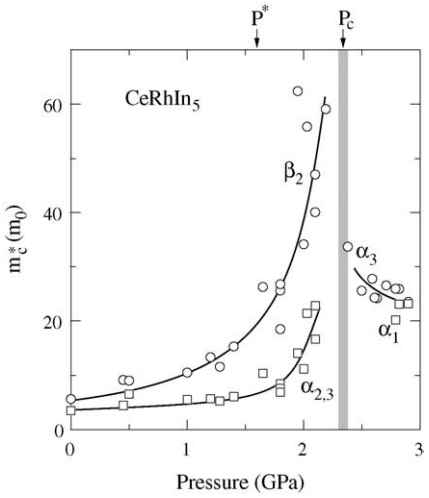

Fig. 7. Pressure dependence of the cyclotron mass in $CeRhIn_5$.

As shown in Fig. 7, the cyclotron masses of main branches β_2 and $\alpha_{2,3}$ increase steeply above 1.6 GPa where superconductivity sets in: $5.5m_0$ at ambient pressure, $20m_0$ at 1.6 GPa and $60m_0$ at 2.2 GPa for branches β_2, where the cyclotron mass was determined in the field range from 100 to 169 kOe, namely at an effective field $H_{\rm eff}$ = 126 kOe. On the other hand, the cyclotron mass of the new branch α_3, which was observed above 2.4 GPa, decreases slightly with increasing pressure: about $30m_0$ at 2.4 GPa and $24m_0$ at 2.9 GPa. Branch β_2 was, however, not detected above 2.4 GPa. This is mainly due to a large cyclotron effective mass close to $100m_0$. We note that the cyclotron mass above 1.6 GPa, including the cyclotron mass in $CeCoIn_5$, is field-dependent as described in Refs. [12,13].

From these experimental results, a critical pressure is determined as $P_c \simeq 2.4$ GPa. The topology of the Fermi surface is thus found to be different between $P < P_c$ ($\simeq 2.4$ GPa) and $P > P_c$. Nevertheless superconductivity is observed in both the pressure regions ranging from 1.6 to 5.2 GPa [11,15]. From the NQR experiment at 1.75 GPa, superconductivity with a d-wave type is found to coexist with the antiferromagnetic state [16], and also from the neutron scattering experiment, the magnetic structure and the magnetic moment are almost unchanged up to 1.63 GPa [17]. It is important to emphasize that the cyclotron masses are extremely large in these pressure regions below P_c as well as above P_c, forming a heavy fermion state. We also note that the upper critical field H_{c2} in superconductivity and a slope of H_{c2} at T_c, $-{\rm d}H_{c2}/{\rm d}T$ at 2.5 GPa for the magnetic field along [0 0 1] (c-axis) are 100 kOe and 150 kOe/K, respectively [11], which are compared to 50 kOe and 110 kOe/K in $CeCoIn_5$ at ambient pressure [13]. This indicates that the electronic specific heat coefficient γ at 2.5 GPa in $CeRhIn_5$ is larger than γ = 1000 mJ/K^2 mol in $CeCoIn_5$.

3.3. $CePt_3Si$

A recently discovered superconductor $CePt_3Si$ with the tetragonal crystal structure possesses unique characteristics [18]. Superconductivity with the transition temperature $T_{sc} = 0.75$ K is realized in the long-range antiferromagnetic state with the Néel temperature $T_N = 2.2$ K. This is in contrast with superconductivity in the previous cerium-based heavy fermion superconductors where superconductivity occurs in the nonmagnetic state or the antiferromagnetically spin-fluctuating state [19].

Moreover, it is noted that $CePt_3Si$ is the first heavy fermion superconductor lacking a center of symmetry in the tetragonal crystal structure. Very recently we have also observed superconductivity in the vicinity of a critical pressure for a ferromagnet UIr without inversion symmetry where a Curie temperature becomes approximately zero [20]. The relation between superconductivity and lack of inversion symmetry is currently an interesting issue.

The topology of the Fermi surface in $CePt_3Si$ is most likely similar to that in $LaPt_3Si$. In fact, one small Fermi surface

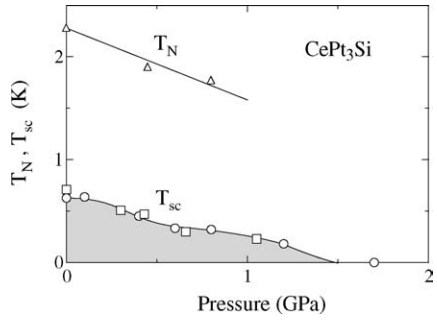

Fig. 8. Pressure dependence of the Néel temperature T_N and the superconducting transition temperature T_{sc} in $CePt_3Si$. The data shown by triangles and circles were obtained by the resistivity measurement, and those by squares are due to the ac-susceptibility one.

named δ ($F = 1.6 \times 10^7$ Oe and $m_c^* = 2.9m_0$) in $CePt_3Si$ is the same as that in $LaPt_3Si$, where the main Fermi surface in $LaPt_3Si$ consists of three-dimensional multiply connected Fermi surfaces [21]. The much larger main Fermi surfaces are not detected experimentally, most likely due to the antiferromagnetic structure in $CePt_3Si$ and the large cyclotron mass of the main Fermi surfaces based on the large electronic specific heat coefficient 300–400 mJ/K^2 mol [18].

We have also carried out the dHvA and electrical resistivity measurements under pressure in $CePt_3Si$. With increasing pressure, the Néel temperature $T_N = 2.3$ K and the superconducting transition temperature $T_{sc} \simeq 0.65$ K are found to decrease markedly, and become zero around 1.5 GPa, as shown in Fig. 8. The corresponding dHvA frequency of branch δ slightly increases in magnitude, while the cyclotron effective mass decreases with increasing pressure: $2.9m_0$ at 0 GPa and $2.4m_0$ at 1.3 GPa. The critical pressure P_c is most likely 1.5 GPa. Above $P_c = 1.5$ GPa another branch $F = 2.20 \times 10^7$ Oe with $m_c^* = 19m_0$ is observed whose cyclotron mass decreases steeply with further increasing pressure.

The heavy fermion state of $CePt_3Si$ is most likely realized at ambient pressure even in the antiferromagnetic state, which is closely related to an appearance of superconductivity. In other words, applying pressure derives the electronic state away from the heavy fermion state and also superconductivity.

4. Concluding remark

We have studied the Fermi surface properties of antiferromagnets $CeIn_3$, $CeRhIn_5$ and $CePt_3Si$ via the dHvA experiments under pressure. The application of pressure to these compounds is useful to control the electronic states. The topology of the Fermi surface is found to be unchanged up to P_c, but an abrupt change of the Fermi surface is observed above P_c for the three compounds. The precise dHvA data are obtained in $CeRhIn_5$. When pressure approaches P_c, the cyclotron mass of the main Fermi surface in $CeRhIn_5$ increases steeply, indicating the heavy fermion state, and decreases considerably when the pressure deviates from P_c. Around P_c, the heavy fermion state is formed, although the topology of the Fermi surface is different between below and above P_c. Namely, the 4f electron is localized below P_c, while the 4f electron becomes itinerant above P_c and contributes to the volume of the Fermi surface. Superconductivity of $CeRhIn_5$ is not related to the topology of the Fermi surface but is closely related to this heavy fermion state. It is also noted that quasi-two-dimensionality enhances the superconducting transition temperature, where $T_{sc} = 0.2$ K in the three-dimensional electronic state of $CeIn_3$ at 2.5 GPa is compared to $T_{sc} = 2.2$ K in $CeRhIn_5$ at 2.4 GPa. Moreover, it is remarkable that the superconducting pressure region ΔP_{sc} is wide in the quasi-two-dimensional electronic state: $\Delta P_{sc} = 0.5$ GPa in $CeIn_3$ and $\Delta P_{sc} = 3.5$ GPa in $CeRhIn_5$.

Acknowledgements

We are very grateful to Prof. Y. Kitaoka for helpful discussions. The present work was financially supported by a Grant-in-Aid for Creative Scientific Research (15GS0213), for Scientific Research of Priority Area and Scientific Research (A) from the Ministry of Education, Culture, Sports, Science and Technology (MEXT). RS was financially supported by the Grant-in-Aid for Scientific Research (C) (14540337) from the MEXT. HS acknowledges the support from the Research Fellowship of the Japan Society for the Promotion of Science for Young Scientists.

References

[1] N.D. Mathur, F.M. Grosche, S.R. Julian, I.R. Walker, D.M. Freye, R.K.W. Haselwimmer, G.G. Lonzarich, Nature 394 (1998) 39.
[2] H. Hegger, C. Petrovic, E.G. Moshopoulou, M.F. Hundley, J.L. Sarrao, Z. Fisk, J.D. Thompson, Phys. Rev. Lett. 84 (2000) 4986.
[3] S. Kawasaki, T. Mito, Y. Kawasaki, H. Kotegawa, G.-Q. Zheng, Y. Kitaoka, H. Shishido, S. Araki, R. Settai, Y. Ōnuki, J. Phys. Soc. Jpn. 73 (2004) 1647.
[4] S. Kawasaki, T. Mito, Y. Kawasaki, G.-Q. Zheng, Y. Kitaoka, D. Aoki, Y. Haga, Y. Ōnuki, Phys. Rev. Lett. 91 (2003) 137001.
[5] T. Ebihara, I. Umehara, A.K. Albessard, K. Satoh, Y. Ōnuki, Physica B 186–188 (1993) 123.
[6] H. Shishido, R. Settai, D. Aoki, S. Ikeda, H. Nakawaki, T. Iizuka, Y. Inada, K. Sugiyama, T. Takeuchi, K. Kindo, T.C. Kobayashi, Y. Haga, H. Harima, Y. Aoki, T. Namiki, H. Sato, Y. Ōnuki, J. Phys. Soc. Jpn. 71 (2002) 162.
[7] T. Yasuda, H. Shishido, T. Ueda, S. Hashimoto, R. Settai, T. Takeuchi, T.D. Matsuda, Y. Haga, Y. Ōnuki, J. Phys. Soc. Jpn. 73 (2004) 1657.
[8] R. Settai, T. Kubo, H. Shishidoa, T.C. Kobayashi, Y. Ōnuki, J. Magn. Magn. Mater. 272–276 (2004) 223.
[9] K. Betsuyaku, H. Harima, J. Magn. Magn. Mater. 272–276 (2004) 187.
[10] R. Movshovich, M. Jaime, J.D. Thompson, C. Petrovic, Z. Fisk, P.G. Pagliuso, J.L. Sarrao, Phys. Rev. Lett. 86 (2001) 5152.
[11] T. Muramatsu, N. Tateiwa, T.C. Kobayashi, K. Shimizu, K. Amaya, D. Aoki, H. Shishido, Y. Haga, Y. Ōnuki, J. Phys. Soc. Jpn. 70 (2001) 3362.

[12] H. Shishido, R. Settai, S. Araki, T. Ueda, Y. Inada, T.C. Kobayashi, T. Muramatsu, Y. Haga, Y. Ōnuki, Phys. Rev. B. 66 (2002) 214510.
[13] R. Settai, H. Shishido, S. Ikeda, Y. Murakawa, M. Nakashima, D. Aoki, Y. Haga, H. Harima, Y. Ōnuki, J. Phys.: Condens. Matter 13 (2001) L627.
[14] S. Ikeda, H. Shishido, M. Nakashima, R. Settai, D. Aoki, Y. Haga, H. Harima, Y. Aoki, T. Namiki, H. Sato, Y. Ōnuki, J. Phys. Soc. Jpn. 70 (2001) 2248.
[15] S. Kawasaki, T. Mito, G.-Q. Zheng, C. Thessieu, Y. Kawasaki, K. Ishida, Y. Kitaoka, T. Muramatsu, T.C. Kobayashi, D. Aoki, S. Araki, Y. Haga, R. Settai, Y. Ōnuki, Phys. Rev. B. 65 (2001) 020504(R).
[16] T. Mito, S. Kawasaki, Y. Kawasaki, G.-Q. Zheng, Y. Kitaoka, D. Aoki, Y. Haga, Y. Ōnuki, Phys. Rev. Lett. 90 (2003) 077004.
[17] A. Llobet, J.S. Gardner, E.G. Moshopoulou, J.-M. Mignot, M. Nicklas, W. Bao, N.O. Moreno, P.G. Pagliuso, I.N. Goncharenko, J.L. Sarrao, J.D. Thompson, Phys. Rev. B. 69 (2004) 024403.
[18] E. Bauer, G. Hilscher, H. Michor, Ch. Paul, E.W. Scheidt, A. Gribanov, Yu. Seropegin, H. Noël, M. Sigrist, P. Rogl, Phys. Rev. Lett. 92 (2004) 027003.
[19] Y. Kitaoka, Y. Kawasaki, T. Mito, S. Kawasaki, G.-Q. Zheng, K. Ishida, D. Aoki, Y. Haga, R. Settai, Y. Ōnuki, C. Geil, F. Steglich, J. Phys. Chem. Solids 63 (2002) 1141.
[20] T. Akazawa, H. Hidaka, T. Fujiwara, T.C. Kobayashi, E. Yamamoto, Y. Haga, R. Settai, Y. Ōnuki, J. Phys.: Condens. Matter 16 (2004) L29.
[21] S. Hashimoto, T. Yasuda, T. Kubo, H. Shishido, T. Ueda, R. Settai, T.D. Matsuda, Y. Haga, H. Harima, Y. Ōnuki, J. Phys.: Condens. Matter 16 (2004) 287.